Plant, Cell and Environment (2006) **29**, 105–114

Dynamics of water transport and storage in conifers studied with deuterium and heat tracing techniques

F. C. MEINZER[1], J. R. BROOKS[2], J.-C. DOMEC[3], B. L. GARTNER[3], J. M. WARREN[1], D. R. WOODRUFF[1], K. BIBLE[4] & D. C. SHAW[4]

[1]*USDA Forest Service, Forestry Sciences Laboratory, 3200 SW Jefferson Way, Corvallis, OR 97331, USA,* [2]*Western Ecology Division, US EPA/NHEERL, 200 SW 35th Street, Corvallis, OR 97333, USA,* [3]*Department of Wood Science and Engineering, Oregon State University, Corvallis, OR 97331, USA and* [4]*Wind River Canopy Crane Research Facility, University of Washington, 1262 Hemlock Road, Carson, WA 98610, USA*

ABSTRACT

The volume and complexity of their vascular systems make the dynamics of long-distance water transport in large trees difficult to study. We used heat and deuterated water (D_2O) as tracers to characterize whole-tree water transport and storage properties in individual trees belonging to the coniferous species *Pseudotsuga menziesii* (Mirb.) Franco and *Tsuga heterophylla* (Raf.) Sarg. The trees used in this study spanned a broad range of height (13.5–58 m) and diameter (0.14–1.43 m). Sap flow was monitored continuously with heat dissipation probes near the base of the trunk prior to, during and following injection of D_2O. The transit time for D_2O transport from the base of the trunk to the upper crown and the tracer residence time were determined by measuring hydrogen isotope ratios in water extracted from leaves sampled at regular intervals. Transit times for arrival of D_2O in the upper crown ranged from 2.5 to 21 d and residence times ranged from 36 to 79 d. Estimates of maximum sap velocity derived from tracer transit times and path length ranged from 2.4 to 5.4 m d^{-1}. Tracer residence time and half-life increased as tree diameter increased, independent of species. Species-independent scaling of tracer velocity with sapwood-specific conductivity was also observed. When data from this study were combined with similar data from an earlier study of four tropical angiosperm trees, species-independent scaling of tracer velocity and residence time with sapwood hydraulic capacitance was observed. Sapwood capacitance is an intrinsic tissue-level property that appears to govern whole-tree water transport in a similar manner among both tracheid- and vessel-bearing species.

Key-words: *Pseudotsuga menziesii*; *Tsuga heterophylla*; capacitance; sap velocity; stable isotopes.

Correspondence: Frederick C. Meinzer. Fax: +1 541 758 7760; e-mail: fmeinzer@fs.fed.us

© 2006 Blackwell Publishing Ltd
No claim to original US government works

INTRODUCTION

Trees typically increase in size by three to four orders of magnitude from the seedling to adult stage. The corresponding increase in the volume and complexity of their vascular systems makes the dynamics of long-distance water transport increasingly difficult to characterize. In the largest trees, transit times for the movement of a given volume of water from roots to leaves in the upper crown may take several days, yet dramatic variations in sap velocity occur over a few minutes. Superimposed on this axial movement of water is the influence of hydraulic capacitance on the repeated exchange of water between storage compartments and the transpiration stream. Thus, to adequately characterize the relationship between tree hydraulic architecture and water movement *in vivo*, multiple techniques with a broad range of spatial and temporal resolutions are required. Heat tracing techniques for measurement of sap flow (e.g. Marshall 1958; Granier 1985; Burgess *et al.* 2001) have the advantage of being able to continuously track variations in flow at relatively precise locations in the xylem. Simultaneous measurements at different depths in stems can be used to construct radial profiles of axial flow (Jiménez *et al.* 2000; James *et al.* 2002; Ford *et al.* 2004). However, circumferential, radial and axial variations in sap flow present challenges for adequate sampling, even in relatively small trees (Nadezhdina, Cermak & Ceulemans 2002). On the other hand, isotope tracers such as deuterated water (D_2O) integrate properties of a larger portion of the vascular system and, if carefully injected and sampled, can reveal much about maximum sap velocity, whole-tree water flux, and storage and retention of water (Waring & Roberts 1979; Calder *et al.* 1992; Dye, Olbrich & Calder 1992; Kalma, Thorburn & Dunn 1998; James *et al.* 2003; Meinzer *et al.* 2003; Marc & Robinson 2004). Nevertheless, the spatial resolution of isotope tracing techniques is relatively poor and they are generally not suited for characterizing water transport dynamics over periods of less than a day. The combined use of heat and isotope tracing techniques can facilitate the integration of whole-tree water transport properties across a range of spatial and temporal scales.

Maximum xylem transport velocities and residence times of water in the xylem have relevance for the relative roles of chemical and hydraulic signalling of conditions in the rhizosphere of tall trees. Hydraulic signals, propagated as changes in xylem tension, provide an essentially instantaneous means of root-to-shoot communication of changes in variables such as soil water status and rhizosphere hydraulic resistance. Indeed, previous work has shown a linear decline in daily maximum stomatal conductance with increasing loss of root hydraulic conductivity resulting from drought-induced embolism in the coniferous species *Pseudotsuga menziesii* and *Pinus ponderosa* (Domec *et al.* 2004) and in several tropical savannah woody species (Domec *et al.* 2005). However, the physiological role of root-to-shoot communication via chemical signals in the transpiration stream of trees remains unclear. A number of studies suggest root-derived abscisic acid as a modulator of stomatal opening in trees subjected to rhizosphere stresses such as soil drying, flooding and compaction (Davies & Zhang 1991). In contrast, other studies suggest that hydraulic signals play a dominant role in the modulation of stomatal responses to rhizosphere stresses in trees (Saliendra, Sperry & Comstock 1995; Fuchs & Livingston 1996). Estimates of sap velocity in conifers obtained through the heat pulse method imply that in the tallest trees, several days would be required for a chemical signal generated in the roots to arrive in the upper crown. Nevertheless, lag times for the arrival of root-derived chemical signals in tall trees may represent less of a constraint on the efficacy of chemical signalling than the lag times for the dissipation of chemical signals, because stresses such as soil drought develop slowly over many days, whereas release from drought after a significant rain event is nearly instantaneous. A previously generated chemical signal would presumably continue to arrive at the foliage of a tall tree for several days after release from drought. Studies of the propagation velocity and dissipation of chemical tracers in the xylem sap of large trees should therefore prove useful in elucidating the relative importance of the hydraulic and chemical control of foliage response to fluctuations in rhizosphere stresses.

Comparative studies of tropical angiosperm trees in which heat and stable isotope tracers have been employed point to species-independent scaling of whole-tree water transport and storage dynamics with the fundamental biophysical properties of sapwood such as hydraulic capacitance and conductivity (James *et al.* 2003; Meinzer *et al.* 2003), or other allometric traits (Andrade *et al.* 1998; Meinzer, Goldstein & Andrade 2001). In the present study, similar heat and isotope tracer techniques were applied to temperate coniferous trees spanning a broad range of sizes. The objectives of this study were to evaluate the extent to which key characteristics of whole-tree water transport and storage were size-dependent, species-independent among conifers, and species-independent among conifers and angiosperms, which differ in the basic structure of their xylem elements (tracheids versus vessels). The latter objective was addressed by comparing data obtained in the present study with data previously obtained from four tropical angiosperm species (James *et al.* 2003; Meinzer *et al.* 2003).

METHODS

Field sites and plant material

The study was carried out at two sites located within 5 km of each other in the Wind River Basin of south-western Washington. The site with the tallest trees was a 450-year-old Douglas-fir [*P. menziesii* (Mirb.) Franco]/western hemlock [*Tsuga heterophylla* (Raf.) Sarg.] forest located at the Wind River Canopy Crane Research Facility (WRCCRF) situated within the T.T. Munger Research Natural Area of the Gifford Pinchot National Forest (Shaw *et al.* 2004). The stand has a mean density of about 427 trees ha^{-1}, with a maximum height of 56–65 m for the dominant trees. The WRCCRF contains a 75-m-tall construction crane with an 85 m jib that provided access to the crowns of the study trees via a suspended gondola. The second site, located in the Wind River Experimental Forest, was clear-cut in 1976 and planted with Douglas-fir seedlings in 1978. During the study period, the mean density was about 1529 trees ha^{-1} with a mean height of about 16 m (McDowell *et al.* 2002; Phillips *et al.* 2002). A 19.5-m-tall scaffold tower provided access to the crowns of the study trees.

The altitudes of the younger and older stands are 561 and 371 m, respectively. The mean annual temperature is 8.7 °C with means of 0 °C in January and 17.5 °C in July. The Pacific maritime climate of the region is characterized by wet winters and dry summers. The mean annual precipitation in the region is about 2.5 m, over 70% of which falls as snow, and a dry season occurs from June through September. Very low precipitation between these months (≈ 119 mm) typically leads to drought conditions in the upper portion of the soil profile, but species such as *P. menziesii* are able to tap increasingly deep sources of soil water as the dry season progresses (Warren *et al.* 2005). Photosynthetic photon flux (PPF) and vapour pressure deficit (VPD) during the course of the study were obtained from data recorded by the WRCCRF at 60 m on the canopy crane tower.

Eight trees, two large individual trees each of *P. menziesii* and *T. heterophylla* accessible from the canopy crane and four individual trees of *P. menziesii* accessible from the scaffold tower in the younger stand, were selected for D_2O injection and sap flow and sapwood capacitance measurements as described further in this paper. Tree characteristics are summarized in Table 1.

Transport of D_2O

A procedure similar to that described by James *et al.* (2003) was used to inject deuterium oxide (99.8 atom % D_2O; Icon Isotopes, Summit, NJ, USA) into the transpiration stream through holes spaced at regular intervals around the circumference of the trunk. About 10–20 mm of bark was first removed with a 50-mm-diameter hole saw, then the remain-

© 2006 Blackwell Publishing Ltd,
No claim to original US government works

Table 1. Characteristics of the eight coniferous trees injected with deuterated water (D_2O). Trees at the Wind River Canopy Crane Research Facility are all tagged and identified by individual numbers, whereas the young trees were assigned numbers for this study

				D_2O tracer				
Species	Height (m)	Diameter (m)	Sapwood area (m^2)	Injected (g)	Arrival (d)	Velocity ($m\ d^{-1}$)	Half-life (d)	Residence (d)
P. menziesii								
Y1	13.5	0.21	0.024	31	2.5	5.4	1.8	36
Y2	13.5	0.17	0.015	25	3.5	3.9	1.6	38
Y3	13.5	0.14	0.012	21	3.5	3.9	1.9	34
Y4	13.5	0.21	0.026	31	2.5	5.4	1.5	44
2108	58	1.43	0.240	213	11.5	5.0	6.4	79
2120	54	1.06	0.132	151	14.0	3.9	9.2	69
T. heterophylla								
260	50	0.93	0.292	135	21	2.4	7.3	61
383	56	0.89	0.268	133	17	3.3	5.1	57

ing bark and the outermost few millimetres of sapwood were removed with a 25-mm-diameter spade bit pointed downward at an angle of about 30° above horizontal and about 1.3 m above ground level. Finally, holes (≈ 5 mm in diameter, ≈ 50 mm deep) were drilled in the centre of the exposed sapwood at an angle of about 30° above horizontal and into the sapwood. Immediately after drilling, each hole was fitted with a reservoir device consisting of flexible tubing passing through a rubber stopper and connected to a plastic syringe barrel. The rubber stopper fit snugly in the cylindrical cavity formed by the removed bark and the end of the flexible tubing rested near the bottom of the hole. The reservoir was filled with D_2O and was refilled periodically as the D_2O was taken up into the transpiration stream. Air displaced by injecting D_2O into the hole was purged through a second piece of flexible tubing that passed through the rubber stopper but not into the injection hole. The D_2O was injected simultaneously through four holes spaced 90° apart in each of the young *P. menziesii* trees, eight evenly spaced holes in the largest *P. menziesii* tree (Tree #2108) and six evenly spaced holes in the remaining trees. Total amounts of D_2O injected were adjusted according to the size of the tree (Table 1), but the dosage was kept constant at ≈ 0.5 g D_2O per cm of sapwood circumference. In the young *P. menziesii* stand, injections began on 9 July 2003 at 1200 h and were completed by 1500 h. In the old-growth *P. menziesii*/*T. heterophylla* stand, injections began on 6 August 2003 at 0900 h and were completed by 1400 h.

Presence of the D_2O tracer in foliage water was detected by periodically collecting needles from the different regions of the upper crown and immediately sealing them in glass vials with polyethylene cone inserts in the cap and then wrapped with Parafilm (American Can Co., Greenwich, CT, USA) to prevent evaporation. Foliage samples were collected prior to D_2O injections to establish baseline hydrogen isotope ratios. Periodic collections then followed the injection, starting with daily sample collections, which eventually shifted to less frequent collections after 10–16 d. Cryogenic vacuum distillation was used in extracting water from the needle samples (Ehleringer & Osmond 1989; Dawson 1993; Ehleringer, Roden & Dawson 2000). Water samples were analysed for hydrogen and oxygen isotope ratios (δD, $\delta^{18}O$) on an isotope ratio mass spectrometer (Delta plus, Finnigan, Bremen, Germany) interfaced with a high-temperature conversion/elemental analyser (TC/EA, ThermoQuest Finnigan, Bremen, Germany) located at the Integrated Stable Isotope Research Facility US Environmental Protection Agency (EPA) Western Ecology Division in Corvallis, OR. All δD and $\delta^{18}O$ values are expressed relative to Vienna Standard Mean Ocean Water (V-SMOW) in ‰, as shown in Eqn 1:

$$\delta D \text{ or } \delta^{18}O = \left(\frac{R_{sample}}{R_{standard}} - 1\right) 1000 \quad (1)$$

where R is the ratio of deuterium to hydrogen atoms or ^{18}O to ^{16}O atoms of the sample and the standard V-SMOW. Measurement accuracy and precision was 1.5 and 2.2‰ for δD, and 0.1 and 0.3‰ for $\delta^{18}O$ as determined by repeated measures on laboratory standards through the processing of these samples. Measurements of $\delta^{18}O$ were used so that δD values enriched from the tracer could be distinguished from δD values enriched from evaporation. Both δD and $\delta^{18}O$ of water become enriched through evaporation, whereas only δD increased with the addition of D_2O.

The behaviour of the D_2O tracer in the trees was used to determine three principal water transport and storage characteristics: tracer velocity, tracer half-life and tracer residence time. Tracer concentrations were normalized with respect to their maximum values for all calculations. Tracer velocity ($m\ d^{-1}$), an estimate of maximum sap velocity, was calculated by dividing the estimated path length from injection point to sampling point by the time required for the tracer to reach ≈ 10% of its maximum concentration above baseline levels. This time interval was estimated by the interpolation between successive sampling dates. Tracer half-life (d) was estimated by fitting an exponential decay function to a plot of the relationship between tracer concentration and time elapsed beginning with maximum concentration set at time = zero, and including three to five successive sampling dates (Eqn 2):

© 2006 Blackwell Publishing Ltd,
No claim to original US government works

$$Y = Y_0 e^{-\lambda t} \quad (2)$$

where Y_0 and Y are the tracer concentrations at time zero and time t, respectively and λ is the decay constant. The half-life, Δt, is obtained by solving for the time required for the tracer concentration to fall to one-half of its maximum value ($\Delta t = -\ln 0.5/\lambda$). Tracer residence time (d) was estimated by linear extrapolation of the latter portion of the tracer concentration time course to the pre-injection deuterium concentration baseline.

Sap flow

Variable length heat dissipation sap flow probes, with a heated and reference sensor measuring length of 10 mm at the probe tip (James *et al.* 2002), were used to determine sap flux at multiple radial depths near the base of the north side of the trunk of each tree listed in Table 1. In *P. menziesii*, probes were installed at radial depths of 1.5, 2.5 and 3.5 cm in young trees, and at 1.5, 3.0, 4.5 and 6 cm in old-growth trees. In *T. heterophylla*, which has deep sapwood, probes were installed at depths of 1.5, 5.5, 9.5 and 15 cm. For probe installation, two 38-gauge (2.58-mm-diameter) holes axially separated by 10 cm were drilled into the sapwood. The sensors were coated with a thermally conductive silicone heat sink compound prior to insertion. All probes were protected from potential sunflecks by reflective insulation. Signals from the sap flow probes were scanned every 1 min and 10 min means were recorded by a data logger (CR10X, Campbell Scientific Corp., Logan, UT) equipped with a 32-channel multiplexer (AM416; Campbell Scientific). Concurrent differential voltage measurements across the copper thermocouple leads were converted to a temperature difference between the heated and reference sensor (ΔT), which was converted to sap flux (J_s; g m^{-2} s^{-1}) using the empirical calibration of Granier (1985) (Eqns 3, 4):

$$J_s = 119\, k^{1.231}, \quad (3)$$

where:

$$k = (\Delta T_m - \Delta T)/\Delta T, \quad (4)$$

and where ΔT_m is the temperature difference when sap flux is assumed to be zero. For comparison of sap flux with the velocity of the D_2O tracer, total daily flux at the outermost probe depth was expressed as a volume per unit sapwood area (m^3 m^{-2} d^{-1}), which yielded units compatible with velocity (m d^{-1}). The mass flow of sap corresponding to each probe (F; g s^{-1}) was calculated as shown in Eqn 5:

$$F = J_s A, \quad (5)$$

where A (m^2) is the cross-sectional area of the sapwood calculated as the ring area centred on the 10-mm-long sensor and extending midway between two sensors of successive depths. The innermost sensor was considered to measure the sap flux to the sapwood inner boundary, which was estimated from the x-intercept of a curve fitted to a plot of J_s versus sapwood depth. Whole-tree water use (kg h^{-1}) was calculated as the sum of the three to four values of F measured along the radial profile.

Sapwood conductivity and capacitance

Specific conductivity (k_s) of the outermost portion of sapwood was estimated as given by Eqn 6.

$$k_s = J_v/(\partial P/\partial x), \quad (6)$$

where the value of J_s is the mean maximum flux at the outermost sensor at midday when capacitance-induced lags in flow at the base of the tree are negligible, and $\partial P/\partial x$ is the corresponding transpiration-induced (frictional) tension gradient in the trunk. Frictional tension gradients were calculated from total tension gradients estimated from predawn and midday pressure chamber measurements on twigs obtained at different heights in previous studies. Midday vertical tension gradients in the old-growth stand were remarkably consistent (≈ 0.017 MPa m^{-1}) among studies carried out in different years (Bauerle *et al.* 1999; Woodruff, Bond & Meinzer 2004). The transpiration-induced component was calculated by subtracting the standing gravitational component (0.01 MPa m^{-1}). Midday values of $\partial P/\partial x$ were 0.01 MPa m^{-1} in the young *P. menziesii* trees and 0.007 MPa m^{-1} in the large individual trees of both *P. menziesii* and *T. heterophylla*.

Sapwood capacitance was determined by using a procedure similar to that described by Meinzer *et al.* (2003). Briefly, cylinders of sapwood were collected from trunks of old-growth *P. menziesii* and *T. heterophylla* and young *P. menziesii* trees with an increment borer at about 1.2 m above ground level. Following hydration overnight in distilled water, the cylinders were cut into 10 mm segments, quickly blotted to remove excess water, placed in caps of thermocouple psychrometer chambers (83 series, JRD Merrill Specialty Equipment, Logan, UT), weighed and then sealed inside the rest of the chamber for measurement of their water potential with a 12-channel digital psychrometer meter (85 series, JRD Merrill Specialty Equipment) after at least 2 h of equilibration. Water potential isotherms were generated by making repeated measurements of the mass and water potential of the samples as they were allowed to slowly dehydrate. Sapwood moisture release curves were generated by plotting water potential against the mass of water released per unit sapwood volume. Sapwood capacitance (kg m^{-3} MPa^{-1}) was estimated as the slope of a linear regression fitted to the nearly linear initial phase of the water release curves between 0 and –1 MPa.

RESULTS

Injection of D_2O had no discernible effect on sap flux above the points of injection (Fig. 1) because the amounts injected were small in relation to the total mass flow of sap. Maximum rates of whole-tree sap flow ranged from 2 to 3 kg h^{-1} in the smaller *P. menziesii* trees to 12 kg h^{-1} in the largest *P. menziesii* tree. There was a strong relationship between maximum δD values of water extracted from upper canopy

© 2006 Blackwell Publishing Ltd,
No claim to original US government works

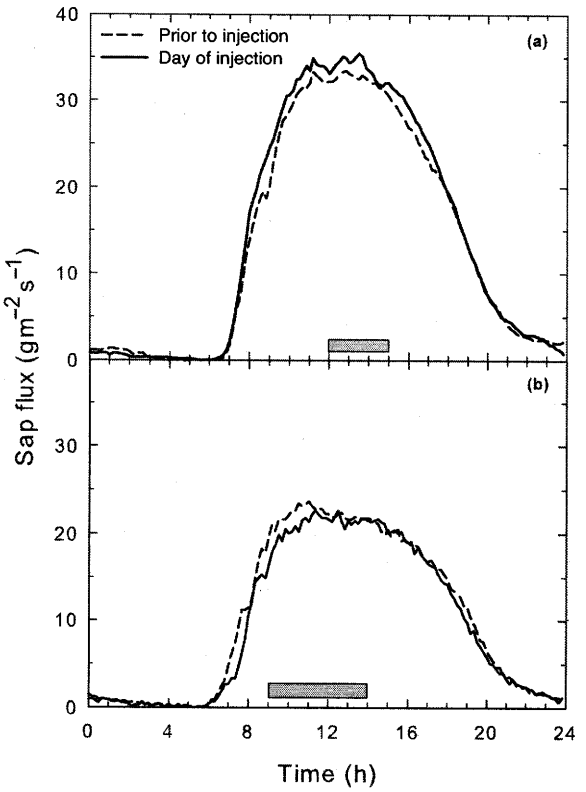


Figure 1. Daily courses of sap flux in the outermost 2 cm of sapwood of *Pseudotsuga menziesii* trees 2 d prior to injection and on the day of injection of pure deuterated water (D_2O). Shaded bars indicate duration of D_2O injections. (a) A 0.21-m-diameter tree injected with 30.8 g D_2O. (b) A 1.43-m-diameter tree injected with 213 g D_2O.

foliage and the amount of tracer injected per unit tree basal area (Fig. 2). Maximum leaf water δD ranged from 110‰ in the largest tree injected (2108) to 2657‰ in the smallest tree injected (Y3). Background δD values of soil and stem water averaged −86 ± 9‰ SD for both stands (δ^{18}O values averaged −10.1 ± 2.3‰ SD). Leaf water near midday showed the typical isotopic enrichment from transpiration with background δD values averaging −37 ± 5‰ SD and δ^{18}O values averaging 6.3 ± 2.9‰ SD.

Environmental conditions in each stand during the tracer experiment are summarized in Fig. 3. In the young *P. menziesii* stand, this period (July) was characterized by clear weather with the exception of one day, and daily maximum VPD was generally between 2 and 3 kPa. Generally clear weather also prevailed in the old-growth stand, except for a 3 d cool cloudy period at the end of the experiment when δD values of foliage water were already close to the pre-injection baseline values. Half-hourly atmospheric VPD exceeded 3 kPa on several days during this 40 d period (August–September).The accumulation of the tracer in the upper crown and its disappearance followed similar types of trajectories in all individuals injected (Fig. 4). After an initial lag, the tracer concentration increased abruptly to a maximum value, then declined

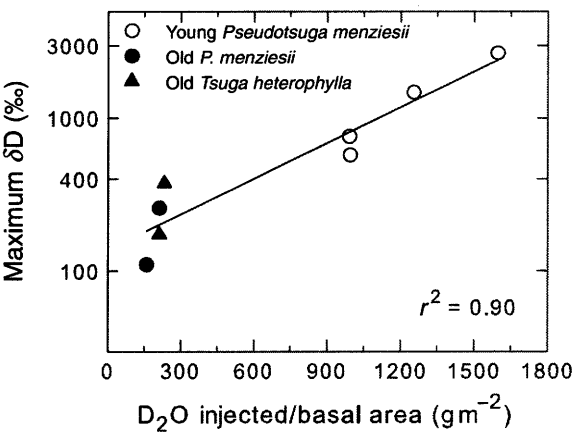


Figure 2. Relationship between maximum deuterium tracer concentration detected in foliage of upper crown and the amount of tracer injected per unit basal area ($\log(y) = 2.14 + 0.000775x$; $P < 0.001$). Average natural abundance δD values for foliage prior to injection were −37‰ ± 5 SD for both stands.

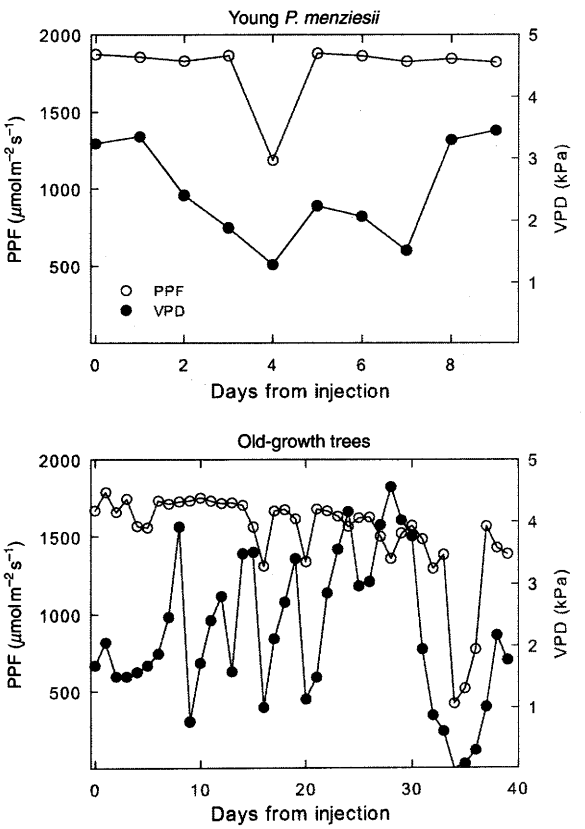


Figure 3. Time courses of maximum daily photosynthetic photon flux (PPF) and atmospheric vapour pressure deficit (VPD) beginning on the day of deuterated water (D_2O) injection and ending when δD values in foliage water had nearly returned to pre-injection baseline levels. Day zero was 9 July in the young stand and 6 August in the old-growth stand.

© 2006 Blackwell Publishing Ltd,
No claim to original US government works

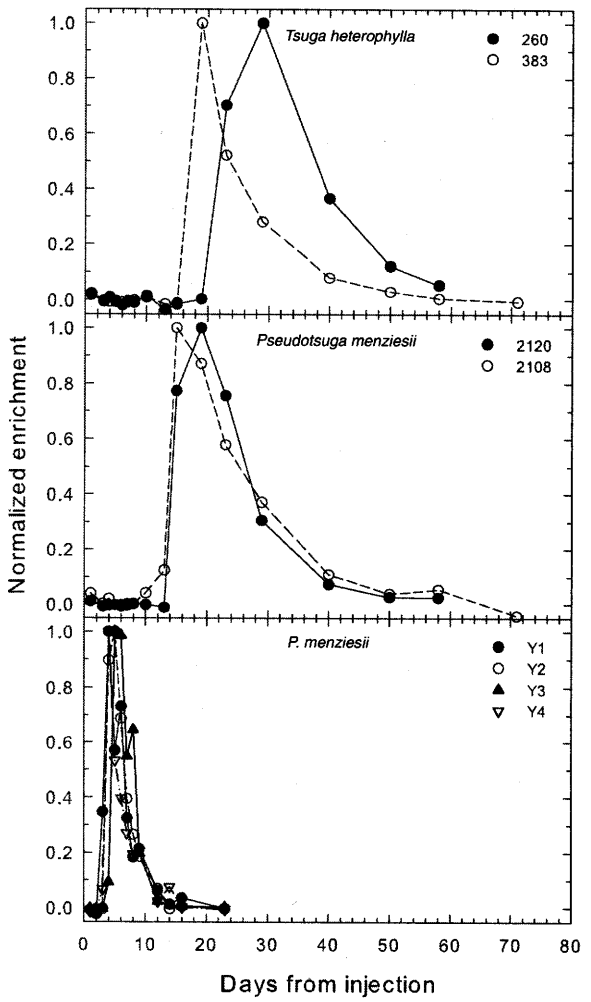


Figure 4. Time courses of normalized δD of water extracted from upper canopy foliage. Tree characteristics are given in Table 1.

more gradually. The time required for the arrival of detectable levels of tracer in the foliage was as short as 2.5 d in the young *P. menziesii* trees to as long as 21 d in the 0.93 m *T. heterophylla* tree (Table 1). When the estimated distances travelled were divided by the transit times, the resulting tracer velocities ranged from a mean of 4.6 m d^{-1} in small and large *P. menziesii* trees to 2.8 m d^{-1} in the large *T. heterophylla* trees. The tracer half-life was less than 2 d in the small *P. menziesii* trees and about 5–9 d in the old-growth trees. Consistent with estimated half-lives, total residence times were shortest in the small trees and longest in the old-growth trees. Tracer half-life and residence time both increased as tree diameter increased, independent of species (Fig. 5). Other measures of tree size were also strongly correlated with tracer half-life and residence time after log transformation to linearize the relationships. These measures included basal sapwood area, an index of tree volume calculated as $\pi r^2 h$, where r is basal radius and h is tree height, and above-ground biomass, estimated from diameter using published species-specific allometric equations. However, none of these measures of tree size was as strong a predictor of tracer dynamics ($r^2 = 0.83$–0.95) as diameter ($r^2 = 0.96$–0.97; Fig. 5), and all involve assumptions about diameter-based tree allometric relationships that were not tested.

There was a positive linear relationship between tracer velocity and total daily sap flux in the outer sapwood where sap flux was highest (Fig. 6). However, tracer velocity was approximately five times greater than sap flux measured with heat dissipation probes. The relationship between sap flux and tracer velocity did not appear to be influenced by tree size or species. Tracer velocity increased along with increased specific conductivity of the outer sapwood estimated from the ratio of sap flux to the transpiration-induced tension gradient (Fig. 7).

Sapwood capacitance normalized on a volume basis was 418 kg m^{-3} MPa^{-1} in the young *P. menziesii* trees, 480 kg m^{-3} MPa^{-1} in the old-growth *T. heterophylla* trees and 518 kg m^{-3} MPa^{-1} in the old-growth *P. menziesii* trees. Because sapwood samples from different individuals were pooled, only one value was available per species or size class. Tracer residence time appeared to increase with sapwood capacitance (cf. Table 1), but no relationship between tracer velocity and capacitance was evident. However,

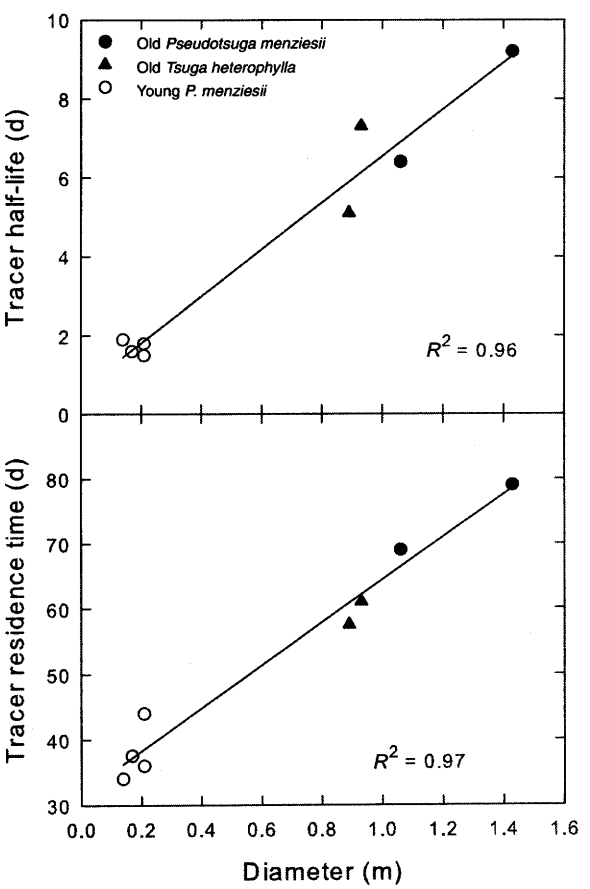


Figure 5. Tracer half-life and residence time in relation to tree diameter.

© 2006 Blackwell Publishing Ltd,
No claim to original US government works

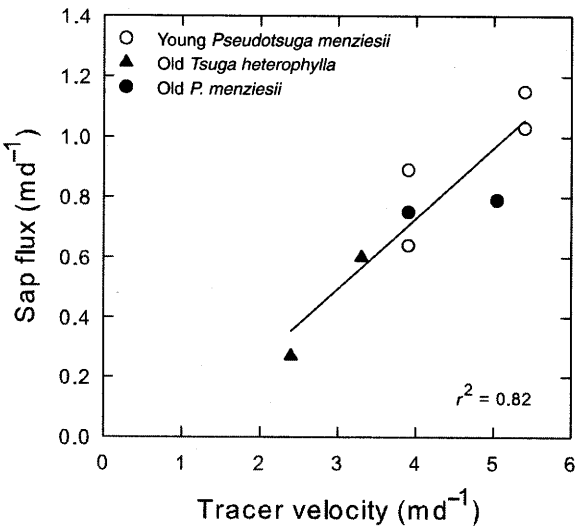


Figure 6. Relationship between tracer velocity and total daily sap flux in the outermost 3 cm of sapwood ($y = -0.21 + 0.23x$; $P = 0.002$).

when sapwood capacitance values, tracer velocities and residence times were combined with the similar measurements previously made on four tropical angiosperm species (James *et al.* 2003; Meinzer *et al.* 2003), highly significant relationships were observed across species (Fig. 8). Tracer velocity declined and residence time increased with increasing sapwood capacitance. Similar relationships were observed ($r^2 = 0.90$–0.95) when tracer velocity and residence time were plotted against values of specific capacitance (ΔRWC/Δwater potential), which were 0.70, 0.73 and 0.65 MPa^{-1} for *T. heterophylla*, old-growth *P. menziesii* and young *P. menziesii*, respectively, and 0.45, 0.34, 0.42 and 0.62 MPa^{-1} for the tropical trees *Anacardium excelsum*, *Cordia alliodora*, *Ficus insipida* and *Schefflera morototoni*, respectively.

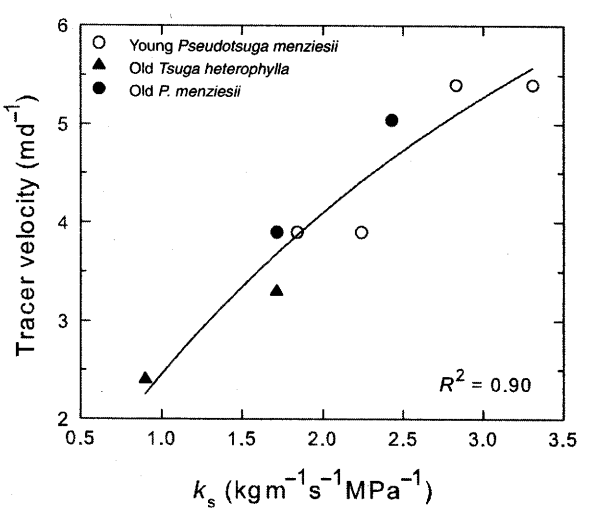


Figure 7. Tracer velocity in relation to specific conductivity of outer sapwood calculated from measurements of sap flux and the frictional water potential gradient as described in the text.

DISCUSSION

Injection of D_2O tracer had no noticeable effect on sap flux above the points of injection, because the mass of the tracer taken up during the 3–5 h of injection was negligible in relation to the total mass of water flowing through the trunk during the same period. In the largest *P. menziesii* tree, about 50 kg of water flowed through the trunk during the same time required for 213 g of D_2O to be taken up. Even in the small *P. menziesii* trees, the mass of D_2O taken up constituted 1% or less of total sap flow during D_2O uptake. The large differences in path length traversed by the tracer from the stem base to upper crown resulted in transit times ranging from as short as 2.5 d in young *P. menziesii* trees to 21 d in a large *T. heterophylla* tree. Tracer transit times and estimated path lengths yielded maximum sap velocities between about 2.5 and 5.5 m d^{-1}. These velocities should be

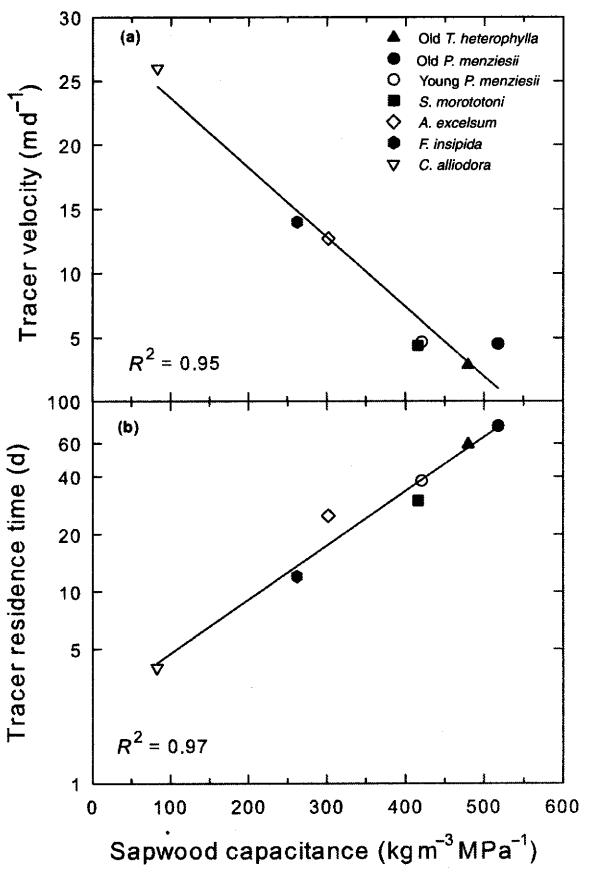


Figure 8. Tracer velocity and residence time in relation to sapwood capacitance of young and old *Pseudotsuga menziesii* trees, old *Tsuga heterophylla* trees and *Schefflera morototoni*, *Anacardium excelsum*, *Ficus insipida* and *Cordia alliodora*, four tropical trees studied by James *et al.* (2003) and Meinzer *et al.* (2003). (a) $y = 29.08 - 0.054x$; $P = 0.002$. (b) log $(y) = 0.387 + 0.00285x$; $P \leq 0.001$.

© 2006 Blackwell Publishing Ltd,
No claim to original US government works

considered as minimum estimates of maximum sap velocity because of the potential for tracer loss via lateral diffusion. Absolute maximum sap velocity was likely to have been higher. There was no apparent difference in tracer velocity between small and large *P. menziesii* trees, but tracer velocities in the two *T. heterophylla* trees were lower than in any of the *P. menziesii* trees. Lower tracer velocity in *T. heterophylla* is consistent with the lower rates of sap flow in *T. heterophylla* than in *P. menziesii*, as measured with heat dissipation probes (Fig. 6 and Moore *et al.* 2004), and may be a consequence of greater sapwood area at a given stem diameter in *T. heterophylla*.

Although estimates of sap flux obtained with independent heat and stable isotope tracing techniques were linearly related (Fig. 6), velocities inferred from heat dissipation measurements were only about 20% of those estimated from transport of D_2O. The range of sap velocity estimated with the heat dissipation technique in the present study is consistent with sap velocities determined for *Pinus contorta* and *Picea engelmanni* using the heat pulse technique (Swanson 1967). It is important to note that only a fraction of the sapwood cross-sectional area consists of conduit lumens. Therefore, true sap velocity is invariably underestimated when heat dissipation measurements of volume flow are normalized by sapwood area in order to obtain velocity units. In the present study, estimates of total daily sap flux increased by about 35% when wood density (≈ 0.42 g cm^{-3} in the individual trees studied) and a cell wall material density of 1.53 g cm^{-3} were used to obtain a multiplier to account for the ratio of lumen area to total cross-sectional area. However, this correction was still insufficient to account for the difference between estimates of sap velocity obtained with the heat and stable isotope tracing methods. It is likely that much of the remaining difference was attributable to the fraction of latewood relative to earlywood across the 1 cm of sapwood spanned by the heat dissipation sensors. In *P. menziesii*, the specific hydraulic conductivity of latewood is about an order of magnitude lower than that of earlywood, which would be expected to result in negligible rates of sap flow through latewood (Domec & Gartner 2002). For example, if 50% of the sapwood traversed by a sap flow sensor consists of latewood, the flow velocity through earlywood would be underestimated by a factor of about two. Finally, maximum rates of sap flow in conifers often occur at about 2 cm from the cambium, with flow often decreasing sharply towards depths on either side of the maximum (Ford *et al.* 2004; Meinzer, Woodruff & Shaw 2004). Thus, flow may not have been maximal at the sensor insertion depths in the present study.

Whole-tree water transport and storage characteristics exhibited species-independent scaling with respect to tree allometric and sapwood biophysical traits. Tracer half-life and residence time scaled in a similar manner with tree basal diameter among all individual trees studied (Fig. 5). The common relationship between D_2O tracer velocity and sapwood-specific conductivity (Fig. 7) was consistent with the relationship between the sap flux measured with heat dissipation probes and the theoretical sapwood-specific conductivity among the four tropical tree species (James *et al.* 2003). These observations imply similar stomatal regulation of xylem tension gradients among co-occurring species to produce similar rates of sap flow at a given value of specific conductivity. Sapwood hydraulic capacitance was similar among the coniferous trees studied precluding its use as a variable for explaining the variation in whole-tree water transport and storage dynamics. However, when the data collected in the present study were combined with similar data collected in earlier studies of tropical angiosperm trees (James *et al.* 2003; Meinzer *et al.* 2003), species-independent scaling of D_2O tracer velocity and residence time with sapwood capacitance was observed (Fig. 8). This striking convergence of water transport and storage dynamics in tracheid- and vessel-bearing species suggests a prominent role for sapwood capacitance in governing whole-tree water relations. The results in Fig. 8 are consistent with sapwood capacitance being an indicator of repeated exchanges of water between storage compartments and the transpiration stream. Thus, greater capacitance presumably both retards the advance of the tracer and increases its residence time in the vascular system. Similarities in the scaling of water transport and storage properties with sapwood capacitance among the temperate conifer and tropical angiosperm species studied belie apparent differences in their relative reliance on discharge and recharge of stored water to partly satisfy daily transpirational requirements. Phillips *et al.* (2003) reported that relative reliance on stored water increased with tree size in *P. menziesii*, whereas Meinzer, James & Goldstein (2004) found that the relative contribution of stored water to the daily water budget of the four tropical angiosperm species represented in Fig. 8 remained constant at about 10%, regardless of tree size. The convergence observed in Fig. 8 was not evident when relationships between tracer residence time and tree height and diameter were examined (data not shown). The tropical angiosperms consistently exhibited shorter residence times at a given height or diameter than the conifers, probably because total sap flux and, therefore, rates of water turnover per sapwood volume, are greater in angiosperms than in conifers at a given tree size (Meinzer *et al.* 2005).

The dynamics of D_2O transport and storage observed in old-growth *P. menziesii* and *T. heterophylla* trees have implications on the use of the oxygen isotope composition of tree rings to assess climate history and variability. In large old-growth trees, the effects of seasonal changes in the isotopic composition of source water on leaf water, and therefore on the isotopic composition of photosynthate incorporated into tree rings, will be greatly attenuated and delayed. The magnitude of this attenuation is inversely related to tree size (e.g. Fig. 5), suggesting that a size function should possibly be incorporated into dynamic models describing the effects of seasonal changes in source water on the isotopic composition of leaf water. This attenuation effect would be particularly important when annual tree rings are finely subdivided (Barbour, Walcroft & Farquhar

© 2006 Blackwell Publishing Ltd,
No claim to original US government works

2002; Verheyden *et al.* 2004) or when leaf compounds are repeatedly sampled through the season (Keitel *et al.* 2003).

Our results may also have implications on the integration of hydraulic and chemical signalling in tall trees. The observed tracer transit times of 11.5–21 d imply a similar delay in the arrival of a chemical signal generated from the roots. Although the study site is subject to prolonged summer drought, rates of soil drying are typically slow (Brooks *et al.* 2005; Warren *et al.* 2005), which may be compatible with the potential role of chemical signals in regulating canopy stomatal behaviour. Nevertheless, stomatal response to hydraulic signals generated during soil drying is likely to be more immediate. The observed D_2O residence times suggest that a root-derived chemical signal would dissipate rather slowly following an event such as drought-breaking summer rains. In contrast, the hydraulic effects of such an event would be sensed rapidly in the canopy. This scenario would not necessarily preclude integration of chemical and hydraulic signalling of rhizosphere environmental conditions. A number of studies have shown that leaf water potential, the end result of hydraulic signalling, governs stomatal sensitivity to leaf abscisic acid concentration (Tardieu & Davies 1993; Tardieu, Zhang & Gowing 1993; Tardieu & Simonneau 1998).

ACKNOWLEDGMENTS

This research was supported by the US Department of Agriculture (USDA) Forest Service Ecosystem Processes Program, The Environmental Protection Agency and the Wind River Canopy Crane Research Facility located within the Wind River Experimental Forest, T.T. Munger Research Natural Area in Washington. The facility is a cooperative scientific venture between the University of Washington, the USDA Forest Service Pacific Northwest Research Station and the Gifford Pinchot National Forest. This manuscript has been subjected to the peer and administrative review of the US EPA, and it has been approved for publication as an EPA document. Mention of trade names or commercial products does not constitute endorsement or recommendation for use.

REFERENCES

Andrade J.L., Meinzer F.C., Goldstein G., Holbrook N.M., Cavelier J., Jackson P. & Silvera K. (1998) Regulation of water flux through trunks, branches and leaves in trees of a lowland tropical forest. *Oecologia* **115,** 463–471.

Barbour M.M., Walcroft A.S. & Farquhar G.D. (2002) Seasonal variation in $\delta^{13}C$ and $\delta^{18}O$ of cellulose from growth rings of *Pinus radiata*. *Plant, Cell and Environment* **25,** 1483–1499.

Bauerle W.L., Hinckley T.M., Čermák J., Kucera J. & Bible K. (1999) The canopy water relations of old-growth Douglas-fir trees. *Trees* **13,** 211–217.

Brooks J.R., Meinzer F.C., Warren J.M., Domec J.-C. & Coulombe R. (2005) Hydraulic redistribution in a Douglas-fir forest: lessons from system manipulations. *Plant, Cell and Environment* doi:10.1111/j.1365-3040.2005.01409.x

Burgess S.S.O., Adams M.A., Turner N.C., Beverly C.R., Ong C.K., Khan A.A.H. & Bleby T.M. (2001) An improved heat pulse method to measure low and reverse rates of sap flow in woody plants. *Tree Physiology* **21,** 589–598.

Calder I.R., Kariyappa G.S., Srinivasalu N.V. & Murty K.V.S. (1992) Deuterium tracing for the estimation of transpiration from trees. Part 1. Field calibration. *Journal of Hydrology* **130,** 17–25.

Davies W.J. & Zhang J. (1991) Root signals and the regulation of growth and development of plants in drying soil. *Annual Review of Plant Physiology and Molecular Biology* **42,** 55–76.

Dawson T.E. (1993) Water sources of plants as determined from xylem-water isotopic composition: perspectives on plant competition, distribution, and water relations. In *Stable Isotopes and Plant Carbon–Water Relations* (eds J.R. Ehleringer, A.E. Hall & G.D. Farquhar), pp. 465–496. Academic Press, San Diego, CA, USA.

Domec J.-C. & Gartner B.L. (2002) How do water transport and water storage differ in coniferous earlywood and latewood? *Journal of Experimental Botany* **53,** 2369–2379.

Domec J.-C., Warren J.M., Meinzer F.C., Brooks J.R. & Coulombe R. (2004) Native root xylem embolism and stomatal closure in stands of Douglas-fir and ponderosa pine: mitigation by hydraulic redistribution. *Oecologia* **141,** 7–16.

Domec J.-C., Scholz F.G., Bucci S.J., Meinzer F.C., Goldstein G. & Villalobos-Vega R. (2005) Diurnal and seasonal variation in root xylem embolism in tropical savanna woody species: impact on stomatal control of plant water status. *Plant, Cell and Environment* doi:10.1111/j.1365-3040.2005.01397.x

Dye P.J., Olbrich B.W. & Calder I.R. (1992) A comparison of the heat pulse method and deuterium tracing method for measuring transpiration from *Eucalyptus grandis* trees. *Journal of Experimental Botany* **43,** 337–343.

Ehleringer J.R. & Osmond C.B. (1989) Stable isotopes. In *Plant Physiological Ecology: Field Methods and Instrumentation* (eds R.W. Pearcy, J.R. Ehleringer, H.A. Mooney & P.W. Rundel), pp. 281–300. Chapman & Hall, London, UK.

Ehleringer J.R., Roden J.S. & Dawson T.E. (2000) Assessing ecosystem-level water relations through stable isotope ratio analyses. In *Methods in Ecosystem Science* (eds R.B.J.O.E. Sala, H.A. Mooney & R.W. Howarth), pp. 181–198. Springer, New York, USA.

Ford C.R., McGuire M.A., Mitchell R.J. & Teskey R.O. (2004) Assessing variation in the radial profile of sap flux density in *Pinus* species and its effect on daily water use. *Tree Physiology* **24,** 241–249.

Fuchs E.E. & Livingston N.J. (1996) Hydraulic control of stomatal conductance in Douglas fir [*Pseudotsuga menziesii* (Mirb) Franco] and alder [*Alnus rubra* (Bong)] seedlings. *Plant, Cell and Environment* **19,** 1091–1098.

Granier A. (1985) Une nouvelle méthode pour la mesure de flux de sève brute dans le tronc des arbres. *Annals of Science Forestry* **42,** 193–200.

James S.A., Clearwater M.J., Meinzer F.C. & Goldstein G. (2002) Heat dissipation sensors of variable length for the measurement of sap flow in trees with deep sapwood. *Tree Physiology* **22,** 277–283.

James S.A., Meinzer F.C., Goldstein G., Woodruff D., Jones T., Restom T., Mejia M., Clearwater M. & Campanello P. (2003) Axial and radial water transport and internal water storage in tropical forest canopy trees. *Oecologia* **134,** 37–45.

Jiménez M.S., Nadezhdina N., Cermak J. & Morales D. (2000) Radial variation in sap flow in five laurel forest tree species in Tenerife, Canary Islands. *Tree Physiology* **20,** 1149–1156.

Kalma S.J., Thorburn P.J. & Dunn G.M. (1998) A comparison of heat pulse and deuterium tracing techniques for estimating sap flow in *Eucalyptus grandis* trees. *Tree Physiology* **18,** 697–705.

© 2006 Blackwell Publishing Ltd,
No claim to original US government works

Keitel C., Adams M.A., Holst T., Matzarakis A., Mayer H., Rennenberg H. & Gebler A. (2003) Carbon and oxygen isotope composition of organic compounds in the phloem sap provides a short-term measure for stomatal conductance of European beech (*Fagus sylvatica* L.). *Plant, Cell and Environment* **26,** 1157–1168.

Marc V. & Robinson M. (2004) Application of the deuterium tracing method for the estimation of tree sap flow and stand transpiration of a beech forest (*Fagus sylvatica* L.) in a mountainous Mediterranean region. *Journal of Hydrology* **285,** 248–259.

Marshall D.C. (1958) Measurement of sap flow in conifers by heat transport. *Plant Physiology* **33,** 385–396.

McDowell N.G., Phillips N., Lunch C., Bond B.J. & Ryan M.G. (2002) An investigation of hydraulic limitation and compensation in large, old Douglas-fir trees. *Tree Physiology* **22,** 763–774.

Meinzer F.C., Goldstein G. & Andrade J.L. (2001) Regulation of water flux through tropical forest canopy trees: do universal rules apply? *Tree Physiology* **21,** 19–26.

Meinzer F.C., James S.A., Goldstein G. & Woodruff D. (2003) Whole-tree water transport scales with sapwood biophysical properties in tropical forest canopy trees. *Plant, Cell and Environment* **26,** 1147–1155.

Meinzer F.C., James S.A. & Goldstein G. (2004) Dynamics of transpiration, sap flow and use of stored water in tropical forest canopy trees. *Tree Physiology* **24,** 901–909.

Meinzer F.C., Woodruff D.R. & Shaw D.C. (2004) Integrated responses of hydraulic architecture, water and carbon relations of western hemlock to dwarf mistletoe infection. *Plant, Cell and Environment* **27,** 937–946.

Meinzer F.C., Bond B.J., Warren J.M. & Woodruff D.R. (2005) Does water transport scale universally with tree size? *Functional Ecology* **19,** 558–565.

Moore G.W., Bond B.J., Jones J.A., Phillips N. & Meinzer F.C. (2004) Structural and compositional controls on transpiration in 40- and 450-year-old riparian forests in western Oregon, USA. *Tree Physiology* **24,** 481–491.

Nadezhdina N., Cermak J. & Ceulemans R. (2002) Radial patterns of sap flow in woody stems of dominant and understory species: scaling errors associated with positioning of sensors. *Tree Physiology* **22,** 907–918.

Phillips N., Bond B.J., McDowell N.G. & Ryan M.G. (2002) Canopy and hydraulic conductance in young, mature and old Douglas-fir trees. *Tree Physiology* **22,** 205–211.

Phillips N.A., Ryan M.G., Bond B.J., McDowell N.G., Hinckley T.M. & Cermák J. (2003) Reliance on stored water increases with tree size in three species in the Pacific Northwest. *Tree Physiology* **23,** 237–245.

Saliendra N.Z., Sperry J.S. & Comstock J.P. (1995) Influence of leaf water status on stomatal response to humidity, hydraulic conductance, and soil drought in *Betula occidentalis*. *Planta* **196,** 357–366.

Shaw D.C., Franklin J.F., Bible K., Klopatek J., Freeman E., Greene S. & Parker G.G. (2004) Ecological setting of the Wind River old-growth forest. *Ecosystems* **7,** 427–439.

Swanson R.H. (1967) Seasonal course of transpiration of lodgepole pine and Engelmann spruce. In *Proceedings of the International Symposium on Forest Hydrology* (eds W.E. Sopper & H.W. Lull), pp. 419–433. Pergamon Press, Oxford, UK.

Tardieu F. & Davies W.J. (1993) Integration of hydraulic and chemical signaling in the control of stomatal conductance and water status of droughted plants. *Plant, Cell and Environment* **16,** 341–349.

Tardieu F. & Simonneau T. (1998) Variability among species of stomatal control under fluctuating soil water status and evaporative demand: modeling isohydric and anisohydric behaviours. *Journal of Experimental Botany* **49,** 419–432.

Tardieu F., Zhang J. & Gowing D.J.G. (1993) Stomatal control by both [ABA] in the xylem sap and leaf water status: test of a model and of alternative hypotheses for droughted or ABA-fed field-grown maize. *Plant, Cell and Environment* **16,** 413–420.

Verheyden A., Helle G., Schleser G.H., Dehairs F., Beeckman H. & Koedam N. (2004) Annual cyclicity in high-resolution stable carbon and oxygen isotope ratios in the wood of the mangrove tree *Rhizophora mucronata*. *Plant, Cell and Environment* **27,** 1525–1536.

Waring R.H. & Roberts J.M. (1979) Estimating water flux through stems of Scots pine with tritiated water and Phosphorous 32. *Journal of Experimental Botany* **30,** 459–471.

Warren J.M., Meinzer F.C., Brooks J.R. & Domec J.-C. (2005) Vertical stratification of soil water storage and release dynamics in Pacific Northwest coniferous forests. *Agricultural and Forest Meteorology* **130,** 39–58.

Woodruff D.R., Bond B.J. & Meinzer F.C. (2004) Does turgor limit growth in tall tress? *Plant, Cell and Environment* **27,** 229–236.

Received 5 May 2005; received in revised form 21 June 2005; accepted for publication 26 June 2005

© 2006 Blackwell Publishing Ltd,
No claim to original US government works